Author Manuscript

Author Manuscript

Author Manuscript

Author Manuscript

HHS Public Access

Author manuscript

Catheter Cardiovasc Interv. Author manuscript; available in PMC 2018 April 12.

Published in final edited form as:

Catheter Cardiovasc Interv. 2015 August ; 86(2): E38–E48. doi:10.1002/ccd.25566.

Intravenous Xenogeneic Transplantation of Human Adipose-Derived Stem Cells Improves Left Ventricular Function and Microvascular Integrity in Swine Myocardial Infarction Model

Soon Jun Hong, MD, PhD[1,2,3,4,6], **Pamela I. Rogers, RLATG**[1,2,3,4], **John Kihlken, BA**[3], **Jessica Warfel, BA**[3], **Chris Bull, BA**[3], **Maja Deuter-Reinhard, BA**[1,2,3,4], **Dongni Feng, BA**[1,2,3,4], **Jie Xie, MD**[1,2,3,4], **Aaron Kyle, PhD**[3], **Stephanie Merfeld-Clauss, BA**[1,2,3,4], **Brian H. Johnstone, PhD**[1,2,3,4], **Dmitry O. Traktuev, PhD**[1,2,3,4], **Peng-Sheng Chen, MD**[1,2,3], **Jonathan R. Lindner, MD**[5], and **Keith L. March, MD, PhD**[1,2,3,4]

[1]Krannert Institute of Cardiology, Indianapolis, IN

[2]Indiana Center for Vascular Biology and Medicine, Indianapolis, IN

[3]Indiana University School of Medicine, Indianapolis, IN

[4]R.L. Roudebush Veterans Affairs Medical Center, Indianapolis, IN

[5]Oregon Health & Science University, Portland, Oregon

[6]Korea University Anam Hospital, Seoul, Korea

Abstract

Objectives—The potential for beneficial effects of adipose-derived stem cells(ASCs) on myocardial perfusion and left ventricular dysfunction in myocardial ischemia(MI) has not been tested following intravenous delivery.

Methods—Surviving pigs following induction of MI were randomly assigned to 1 of 3 different groups: the placebo group (n=7), the single bolus group (SB)(n=7, 15×10^7 ASCs), or the divided dose group (DD)(n=7, 5×10^7 ASCs/day for three consecutive days). Myocardial perfusion defect area and coronary flow reserve (CFR) were compared during the 28-day follow-up. Also, serial changes in the absolute number of circulating $CD4^+$T and $CD8^+$T cells were measured.

Results—The increases in ejection fraction were significantly greater in both the SB and the DD groups compared to the placebo group (5.4±0.9%, 3.7±0.7%, and -0.4±0.6%, respectively), and the decrease in the perfusion defect area was significantly greater in the SB group than the placebo group (-36.3±1.8 and -11.5±2.8). CFR increased to a greater degree in the SB and the DD groups than in the placebo group (0.9±0.2, 0.8±0.1, and 0.2±0.2, respectively). The circulating number of $CD8^+$T cells was significantly greater in the SB and DD groups than the placebo group at day 7(3,687±317/μL, 3,454±787/μL, and 1,928±457/μL, respectively). The numbers of small vessels

Correspondence to: Keith L. March MD, PhD, Indiana Center for Vascular Biology and Medicine, 975 W Walnut St, IB441, Indianapolis, IN 46202, Tel: 317-278-0130, Fax: 317-278-0089, kmarch@iupui.edu.

DISCLOSURES

All authors have nothing to disclose related to this experiment.

Author Manuscript Author Manuscript Author Manuscript Author Manuscript

were significantly greater in the SB and the DD groups than the placebo group in the peri-infarct area.

Conclusions—Both intravenous SB and DD delivery of ASCs are effective modalities for the treatment of MI in swine. Intravenous delivery of ASCs, with its immunomodulatory and angiogenic effects, is an attractive noninvasive approach for myocardial rescue.

Keywords

adipose stem cell; intravenous injection; myocardial perfusion; myocardial infarction; ventricular dysfunction

INTRODUCTION

Ischemic heart disease is the leading cause of death in the United States in spite of rapid advances in the treatment of coronary artery disease.(1) The concept of using stem and progenitor cells isolated from adult tissues to treat patients with myocardial ischemia (MI) is gaining momentum. Several clinical trials involving skeletal myoblasts,(2,3) bone marrow-derived progenitor cells,(4-6) and peripheral blood progenitor cells(7,8) have shown encouraging results for limiting myocardial damage and improving myocardial function. Therapies employing adipose-derived stem cells (ASCs) have also emerged as a practical approach to promote recovery. ASCs are mesenchymal cells that share many properties in common with bone marrow-derived mesenchymal stem cells (MSCs), and reside in the stromal-vascular fraction of adipose tissue.(9-11) Therapeutic use of autologous ASCs for cardiac repair is particularly practical due to the ready availability of these cells in large quantities for therapeutic injection. Many studies have employed invasive techniques to deliver stem or progenitor cells directly into a coronary artery or the myocardium. Our recent data demonstrating that ASC delivered intravenously had systemic activity, including effects on bone marrow progenitors and adipose tissue mass as well as pulmonary endothelium,(12) suggested the hypothesis that intravenous ASC delivery would also be a particularly feasible approach to the early provision of stem cells in acute MI, and would demonstrate significant rescue of myocardial function and perfusion without a need for targeted delivery. In the current study, we observed the distribution of intravenously injected human ASCs 2 hrs, 14 days, and 28 days after inducing MI in swine. We then investigated the efficacy of single bolus vs. 3 consecutive divided intravenous injections of human ASCs following induction of MI.

METHODS

Animal Model

Animal handling followed the recommendations of the National Institutes of Health (NIH) guide for the care and use of laboratory animals. The study protocol was approved by the Institutional Animal Care and Use Committee at the Indiana University School of Medicine.

Twenty seven pathogen-free (Michigan State University) Yorkshire cross domestic pigs (28 to 38 kg) of mixed gender were employed. MI was induced by angioplasty balloon inflation in the mid left anterior descending coronary artery (LAD). Pigs surviving acute MI were

Author Manuscript Author Manuscript Author Manuscript Author Manuscript

randomly assigned to 1 of 3 groups: placebo (n=7, 3 mL PBS), single bolus (n=7, 15×10^7 hASCs), or divided dose (n=7, 5×10^7 hASCs/day for three consecutive days) (Fig. 1). To examine hASC distribution and persistence, two pigs were sacrificed 2 hrs and 14 days after systemic injection of 15×10^7 hASCs.

Aspirin 325 mg and clopidogrel 75 mg were given orally 24 hrs prior to anterior MI, followed by aspirin 81 mg daily. Unfractionated heparin (300U/kg) was administered intravenously and repeated to maintain the ACTe300 sec. General anesthesia was induced by intramuscular telazol (4.4 mg/kg), xylazine (2.2 mg/kg), ketamine (2.2 mg/kg) and atropine (0.05 mg/kg). The animal was then intubated and ventilated with a closed volume cycle respirator, and anesthesia maintained with isoflurane (1.5~2.5%) and oxygen (2 L/min) while maintaining euthermia. Buprenex (0.01mg/kg) was administered for analgesia.

Myocardial Infarction Induction and Intracoronary Doppler Measurements

Arterial access was obtained via the femoral artery with a cutdown technique. Left coronary angioplasty was performed using a 7F Hockey-stick guiding catheter (Boston Scientific Corp., Natick, MA). Continuous hemodynamic monitoring was performed via an 8F femoral artery sheath. After baseline left coronary angiography, MI was induced by inflating a Quantum Maverick® 3.5× 8 mm over-the-wire balloon (Boston Scientific Corp.) for 60 minutes in the LAD immediately distal to the first dominant septal perforator. To minimize ventricular arrhythmias, intravenous amiodarone was administered prior to balloon inflation (75 mg/10 min) and continued at 1 mg/min for 60 min post occlusion.(13) Breakthrough arrhythmias were terminated with DC cardioversion when necessary (Medtronic, Minneapolis, MN). Coronary angiography was performed again after balloon inflation and at euthanasia. Serum cardiac troponin-I was measured 48 hrs after MI by chemiluminescent immunoassay (Immulite®, Siemens AG, Munich, Germany) validated for a porcine model (ANTECH® Diagnostics Inc., Morrisville, NC).

Coronary microvascular flow was measured by intracoronary Doppler wire (Flowire, Volcano Corp, Rancho Cordova, CA) at baseline and 2 hr post-MI. Nitroglycerin 0.2 mg was injected into the intracoronary circulation to achieve maximal epicardial coronary artery dilation without significantly affecting coronary microcirculation. A Doppler guidewire was positioned in the LAD just distal to the first dominant septal perforator. The average peak flow velocity was measured at baseline and during maximal hyperemia induced by intracoronary bolus injection of 30 μg adenosine.(14,15) Doppler measurements were repeated at least three times, and the averaged. As a surrogate for microvascular integrity, coronary flow reserve (CFR) was determined as the adenosine-induced average peak flow velocity divided by the baseline average peak flow velocity; this was repeated 28 days later with an identically positioned Doppler wire, as confirmed by two orthogonal views.

Isolation and Culture of Human Adipose Stromal Cells

Human subcutaneous abdominal adipose tissue samples were obtained from 2 female volunteers (age 23 and 38) undergoing liposuction. ASCs isolated from each volunteer were evenly distributed between the single bolus and divided dose groups. Adipose tissue was agitated in 1 mg/ml Collagenase Type I (Worthington Biochemical, Lakewood, NJ) prepared

Author Manuscript Author Manuscript Author Manuscript Author Manuscript

in DMEM/F12 medium (Invitrogen, Carlsbad, CA), supplemented with 10% FBS, 100 units/mL penicillin and 100 μg/mL streptomycin, for 2 hours at 37°C followed by centrifugation at 300g for 8 minutes to separate the stromal cell fraction (pellet) from adipocytes.(16) The pellet was resuspended in DMEM/F12 medium supplemented with 10% FBS filtered through 250 μm Nitex (Sefar America Inc., Kansas City, MO) and centrifuged at 300g for 8 minutes. To eliminate erythrocytes the pellet was treated with RBC lysis buffer (154 mM NH_4Cl, 10 mM $KHCO_3$, 0.1 mM EDTA) for 10 minutes. The final pellet was resuspended and cultured in EGM-2MV media (Cambrex, East Rutherford, NJ). ASC monolayers were passaged when 60-80% confluent and used at passage 3-4. Cell viability was evaluated by Trypan blue staining. For single bolus 15×10^7 hASCs injection, cells were resuspended in 9 mL of PBS with 100U/mL unfractionated heparin and autologous swine serum (450 μL) immediately before delivery, and injected 2 hours post-MI. For the divided dose 5×10^7 hASCs group, cells were resuspended in 3 mL of PBS with 100U/mL unfractionated heparin and autologous swine serum (150 μL) immediately before delivery; ASCs were injected 2, 24, and 48 hours after MI. The suspension was infused at 2 mL/min via ear vein catheter.

Contrast-Enhanced Echocardiography and Myocardial Perfusion Echocardiography

Contrast-enhanced 2D and 3D echocardiography and myocardial contrast echocardiography (MCE) were performed prior to MI, 2 days after MI, and prior to sacrifice at day 28. Pigs were anesthetized with isoflurane and imaged in right lateral decubitus position using a phased-array (S5-1, 1~5 MHz) and matrix-array (X3-1, 1~3 MHz) transducer connected to an iE33 system (Philips Medical System, Andover, MA). Microbubbles were prepared by sonication of a gas-saturated aqueous suspension of distearoylphosphatidylcholine (2 mg/mL) and polyoxyethylene-40-stearate (1 mg/mL)(17), and were intravenously infused during 3D image acquisition using harmonic imaging to optimize left ventricular (LV) endocardial border delineation (Supplemental Fig. 1A,B). The endocardial border at end-systole and end-diastole was manually traced in the 4 chamber apical view from 3D images, and LV end-diastolic volume, end-systolic volume, stroke volume, and ejection fraction (EF) were obtained (Supplemental Fig. 1C~E). Wall thickening and fractional shortening were measured from 2D-guided M-mode recordings (Supplemental Fig. 2A~D). For additional quantification of wall motion, the 16-segment model was used, adding segmental wall motion scores of 1=normal, 2=hypokinesis, 3=akinesis, and 4=dyskinesis (Supplemental Fig. 2E).(18,19) Wall motion score index (WMSI) was calculated as the sum of the scores of the segments divided by the number of the segments evaluated. Data were analyzed by two readers who were blinded to the randomization using QLab software (Version 7.0, Philips Medical System, Andover, MA). Interobserver correlation was 0.82 (P<0.001), and intraobserver correlation on 15 randomly selected cases were 0.89 and 0.84 (P<0.001 for both) for the two readers.

To assess myocardial perfusion, a microbubble suspension (5×10^7 mL^{-1}) was infused intravenously at 1.5 $mL \cdot min^{-1}$ to produce myocardial opacification with minimal inferior wall attenuation. MCE was performed in the parasternal short-axis plane just below papillary muscle level using power modulation at a mechanical index of 0.16. End-systolic images were acquired after a 5-frame high-power (mechanical index 1.2) sequence. The percent area

Author Manuscript Author Manuscript Author Manuscript Author Manuscript

of microbubble perfusion was measured with ImageJ software (1.43u, National Institute of Health, USA). The area at risk (AAR) during LAD coronary occlusion and the region void of perfusion at 2 and 28 days after MI were each measured by two blinded readers, averaged, and expressed as percentages of the total LV area. Interobserver correlation for AAR measurements was 0.81 (P<0.001) and intraobserver correlation for 15 randomly selected cases was 0.86 and 0.82 (P<0.001 for both).

Analysis of Lymphocyte, Monocyte, and Granulocyte Populations in Peripheral Blood

Blood samples were obtained and collected into test tubes containing heparin pre-MI, and day 2, 7, and 28 post-MI. Within 1 hr of collection, peripheral blood mononuclear cells (PBMNCs) were isolated by density gradient centrifugation using Ficoll-Paque plus® (Amersham Biosciences Corp., NJ). The number of lymphocytes, monocytes, and neutrophils in PBMNCs were measured using Coulter LH®755 automated hematology analyzers (Beckman Coulter Inc., CA). Erythrocytes were lysed by incubating in 10 mL of red blood cell lysis buffer solution (154 mM NH_4Cl, 10 mM $KHCO_3$, 0.1 mM EDTA). Lymphocyte subsets analyzed were helper T cells ($CD3^+CD4^+$) or cytotoxic T cells ($CD3^+CD8^+$). Cells were stained with fluorochrome-conjugated monoclonal antibodies against CD8-PE (BD, Franklin Lakes, NJ), CD3-FITC (BD), and CD4-PE (BD) for 20 min at 4°C. Pelleted leukocytes were fixed in 2% paraformaldehyde and analyzed by flow cytometry (BD). Expression levels were analyzed using CellQuest™ Pro software (BD).

DNA Isolation and Real-Time PCR Assays for Alu Sequences

Heart, lung, liver, pancreas, spleen, kidney, and bone marrow were isolated and stored at -80°C. Samples (25 mg) were thawed and homogenized with a BeadBeater-8 (Biospec, Bartlesville, OK). A DNA extraction kit was used for DNA isolation (QIAGEN, Valencia, CA). Standard curves were generated for PCR by addition of known numbers of hASCs ($0\sim10^5$) into pig tissue samples prior to homogenization. Real-time PCR assays for Alu sequences(20) were performed in a reaction volume of 50 μL that contained 25 μL Taqman Universal PCR Master Mix (Applied Biosystems, Foster City, CA), 900 nM each of the forward (5’-CAT GGT GAA ACC CCG TCT CTA-3’) and reverse primers (5’-GCC TCA GCC TCC CGA GTA G-3’), 250 nM TaqMan probe (5’-FAM-ATT AGC CGG GCG TGG TGG CG-TAMRA-3’), and 200 ng target template. Reactions were incubated at 50°C for 2 min and 95°C for 10 min, followed by 40 cycles at 95°C for 15 s and 60°C for 1 min. Cycle-dependent amplification for each tissue sample was used to estimate the number of hASCs. All real-time PCR assays were performed in duplicate and average values presented.

Statistical Analysis

Continuous variables are presented as mean±SEM. Variables measured repeatedly were compared using repeated-measures ANOVA. Kruskal-Wallis test or one-way ANOVA with Tamhane posthoc analysis was used for multiple comparisons. Mann-Whitney U test was used to compare 2 groups, and Spearman’s correlation was calculated with SPSS® 12.0 software (SPSS Inc, Chicago, IL). P <0.05 was considered statistically significant.

Staining and Post-MI Electrocardiographic Monitoring are found in the Detailed Supplemental Methods

Author Manuscript Author Manuscript Author Manuscript Author Manuscript

RESULTS

Study Animals

No significant difference in body weights were noted among the 3 groups at baseline (Table 1). Ventricular tachycardia or fibrillation occurred during each LAD occlusion. Intractable ventricular fibrillation with unsuccessful cardioversion occurred in 4 pigs, and another 2 pigs died suddenly within 48 hrs after MI (22% cumulative attrition rate). Cardiac troponin-I levels were increased in all pigs 48 hrs after MI without significant differences among 3 groups (Table 1).

Changes in Left Ventricular Function

LVEF showed no significant difference among 3 groups before and 2 days after MI. However, LVEF was significantly greater in the single bolus group compared to the placebo group 28 days after MI (Table 1). The changes in LVEF between 2 and 28 days after MI showed significant increases in both the single bolus and the divided dose groups compared to the placebo group (Table 1). While no significant differences were noted in inferior wall thickening during the 28 day follow-up, anterior wall thickening (%) was significantly greater in the single bolus group compared to the placebo group (Table 1; Supplemental Fig. 2B,C). After normalizing anterior wall thickening (%) with inferior wall thickening (%), anterior and inferior wall thickening ratio at day 28 was greater in the single bolus group compared to the placebo group (Table 1). WMSI was similar among 3 groups at Day 2, but WMSI was significantly lower in the single bolus (P=0.002) and the divided dose groups (P=0.002) than the placebo group at day 28 (Supplemental Fig. 2F).

Myocardial Microvascular Perfusion and Coronary Flow

The mean AAR, illustrated in Supplemental Fig. 3A, was 29.7±2.3% in the single bolus group and was not different between groups, and the mean perfusion defect area in the single bolus group decreased from 25.0±1.7% at Day 2 to 14.3±1.3% at Day 28 (Supplemental Fig. 3B). The perfusion defect area (%) at day 28 revealed a strong correlation to the nonviable myocardial area (%) in TTC staining (r=0.81, P<0.001) (Supplemental Fig. 3C,D). When the change in perfusion defect area from day 2 to day 28 was normalized with the AAR, the decrease (improvement) in the perfusion defect area was significantly greater in the single bolus group compared to the placebo group (-36.3±1.8 and -11.5±2.8, P=0.021, respectively) (Fig. 2).

CFR decreased considerably in all 3 groups 2 hours after MI, while the values of CFR at day 28 were significantly greater in the single bolus and the divided dose groups compared to the placebo group (2.3±0.1, 2.1±0.1, and 1.6±0.1, respectively) (Fig. 3A). When the changes in CFR from 2 hr post-MI to day 28 were compared, the increases in the CFR were significantly greater in the single bolus and the divided dose groups than the placebo group (0.9±0.2, 0.8±0.1, and 0.2±0.2, respectively) (Fig. 3A). Moreover, the decreases in the perfusion defect area (%) during the 28 day interval correlated with the increases in CFR (r= -0.71, P=0.001) (Fig. 3B).

Author Manuscript Author Manuscript Author Manuscript Author Manuscript

Immune Modulation

No significant differences in total neutrophil, monocyte, or lymphocyte numbers were observed among groups before or after MI (Supplemental Fig. 4A~D). However, analysis of subpopulations revealed that absolute numbers of $CD8^+$T cells dropped significantly post-MI in the placebo group at day 7 (1,928±457/μL in the placebo group, 3,687±317/μL in the single bolus group, and 3,454±787/μL in the divided dose group) (Supplemental Fig. 4E,F), contributing to a significant increase in the CD4+/CD8+ T cell ratio seen in the placebo group but suppressed in the single bolus and divided dose groups (175±17, 88±5, and 98±16, respectively) (Fig. 4).

Electrical Ventricular Stability after MI

Most PVCs occurred within 10 hours post-MI (Fig. 5), and administration of ASC resulted in significant suppression of PVCs per total beats (%) in the divided dose group when compared with the placebo group at 5 hours (3.8±0.4% and 5.3±0.2% respectively), 6 hours (2.7 ± 0.3% and 5.0±0.4% respectively), and 7 hours post-MI (2.2±0.2% and 4.1±0.1% respectively) (Fig. 5). Also, significant decrease in PVCs (%) was noted in the single bolus group vs. the placebo group 7 hour post-MI (2.7±0.4% and 4.1±0.1% respectively) (Fig. 5).

Comparison of Angiogenesis and Nerve Sprouting

Significant increases in the number of SMA+ small vessels were found in the single bolus group when compared to the placebo group in non-infarct (49±3/mm^2 and 38±5/mm^2, respectively), peri-infarct (40±5/mm^2 and 25±3/mm^2, respectively), and infarct areas (28±4/mm^2 and 15±2/mm^2, respectively) (Fig. 6A,B)(Supplemental Fig. 5A~C). Also, significant increases in the number of SMA+ small vessels were noted in the divided dose group when compared to the placebo group in both peri-infarct (42±4/mm^2 and 25±3/mm^2, respectively) and infarct areas (27±2/mm^2 and 15±2/mm^2, respectively) (Fig. 6A). No significant difference in the number of SMA+ large vessels was found among the groups (Fig. 6B).

Remarkable increases in GAP43+ nerve density were found in the single bolus group (P=0.031) and the divided dose group (P=0.005) when compared to placebo in the peri-infarct areas (Fig. 6C)(Supplemental Fig. 5D~F). No significant difference in the GAP43+ nerve density was found among 3 groups in the non-infarct areas. The most active angiogenesis and nerve sprouting in the single bolus and the divided dose group occurred in the basal, mid-anteroseptal, and anterolateral segments, corresponding to regions where perfusion by MCE increased from day 2 to day 28. Serial sections demonstrated that GAP43+ nerve sprouting were found most prominently around SMA+ small vessels in the peri-infarct areas (Supplemental Fig. 5G~I).

Tissue Distribution of hASCs after Systemic Injection

Real-time PCR for human DNA Alu elements was examined in multiple tissues 2 hour, 14 and 28 days after 15×10^7 hASC injection. Heart was sectioned into 5 short-axis slices each with 4 or 6 segments (Supplemental Fig. 2E), and samples from heart, lung, liver, kidney, pancreas, spleen, and bone marrow were examined for hASC presence. Two hours after intravenous injection, most (85.7%) hASCs were detected in the lungs (Fig. 7A), where

Author Manuscript Author Manuscript Author Manuscript Author Manuscript

ASC numbers decreased significantly 14 days after cell injection. A few hASCs were detected in the peri-infarct area 2 hours after systemic injection of 15×10^7 cells (Fig. 7B), but no hASC were found at day 28 (Fig. 7C). hASCs were also readily visualized in lung 2 hours after systemic injection but not at day 28 (Fig. 7D, E).

DISCUSSION

This is the first study to evaluate the time course of LV contractile function and microvascular integrity after intravenous delivery of human ASCs in a swine MI model. We have demonstrated the feasibility of xenogeneic transplantation of ASCs in the absence of specific immunosuppression, and shown for the first time that intravenous ASC injection either as a single bolus or divided dose (over 3 consecutive days) improves LVEF and CFR, and significantly reduces the extent of myocardial infarction at a 28 day follow-up. We propose that modulation in inflammation manifested by the $CD4^+/CD8^+$T cell ratio, as well as the increase in local angiogenesis and myocardial nerve sprouting after MI contribute to limitation in infarction, with improvement in myocardial and microvascular function. Although most intravenously injected ASCs were trapped in the lung and disappeared within 14 days after cell injection, the beneficial effects persisted at day 28. We hypothesize that intravenous injection of ASCs could be utilized as a potential therapeutic option in patients with MI.

Although many pre-clinical and clinical trials have explored intracoronary, endocardial, or epicardial routes for delivery of stem cells after ischemic myocardial damage (2-7,21,22), these methods of delivery are more invasive than intravenous delivery of stem cells. However, many studies demonstrating functional benefits of invasive cell delivery do not have well-documented data regarding the fate of those delivered cells.(2-7,23) In our previous study, we delivered PBMNCs via intracoronary, epicardial, and retrograde coronary venous routes, and noted that even with these local delivery routes, most delivered PBMNCs were found in the lung within 1 hour after cell delivery(13); this prompted us to hypothesize that cells distributed to the lung might in fact contribute significantly to the beneficial effects observed in numerous studies. Our recent study of intravenous ASC delivery in a mouse model of COPD clearly demonstrated effects of the cells on multiple tissues, including lung, bone marrow, and fat.(12) This effect has also been suggested to explain cardiac effects of bone-marrow derived MSCs, which were shown to secrete factors such as TSG-6 while entrapped in lung tissue following systemic delivery,(20) and more recently also were shown to modulate lung pathology via TSG-6 secretion.(24) Paracrine effects by delivered cells probably played an important role in inhibiting further myocardial damage or progression of cardiac remodeling in the early period after ischemic myocardial damage in these cardiac studies.(2-7,23) The outcomes of this study support the notion that ASCs which lodge in the pulmonary circulation secrete paracrine factors that are delivered directly to the LV on their first-pass, where they produce cardioprotective effects. In our pilot experiment with rat myocardial infarction model, injecting cell-free supernatant from the cultured hASC monolayers containing factors such as VEGF, HGF, TGF-beta, and bFGF did not improve left ventricular function as prominent as giving hASCs intravenously (Supplemental Fig. 6). We assume that even though intravenously injected hASCs disappear within 2 weeks from pulmonary vessels, injected hASCs continuously secrete angiogenic and anti-apoptotic

Author Manuscript Author Manuscript Author Manuscript Author Manuscript

factors into circulation in the early period after myocardial ischemia, thereby demonstrating significant improvement in left ventricular function after myocardial damage in this study.

LV remodeling, which includes infarct expansion and LV dilatation, starts very early after MI,(25-28) and is an indication of poor prognosis and occurs despite coronary revascularization.(26) While end-diastolic and end-systolic volumes increased post-MI in the placebo group, these adverse changes were remarkably ameliorated in the single bolus group during the 28 day follow-up after MI, with more prominent decreases in the end-systolic volume, indicating beneficial effects of early intravenous ASC injection on both systolic function and LV remodeling in this study (Supplemental Fig. 1C,D). Significant functional improvement in stroke volume was observed in the single bolus group when compared to the placebo group at day 28, indicating beneficial effects of early intravenous ASC injection in LV contractile function (Supplemental Fig. 1E).

MCE is a useful technique for evaluating myocardial microvascular perfusion during acute coronary occlusion, as well as eventual infarct size. We demonstrated a significant reduction in the post-MI perfusion defect in animals receiving single bolus ASCs (Fig. 2, Supplemental Fig. 3B). This study also showed the expected correlation between the perfusion defect area (%) and the nonviable myocardial area in TTC staining (%) ($r=0.81$, $P<0.001$), suggesting that improvement in vascularization in border zones resulted in smaller infarct size. Moreover, the decreases in the perfusion defect area (%) during the follow-up correlated with the increases in CFR ($r=-0.71$, $P=0.001$) which indicate that the decreases in perfusion defect area indeed represent improvement in myocardial microvascular flow. Nerve sprouting and angiogenesis contribute to the improvement in LV contractile function and microvascular flow, and significant increases in the nerve density and the number of ±-actin^{+} small vessels colocalized at the border where perfusion by MCE increased during the follow-up in the ASC injected groups (Supplemental Fig. 5). This suggests that real-time MCE could be used as a valuable noninvasive tool to evaluate angiogenesis induced by ASC delivery in clinical practice.

T cells play an important role in regulating the early inflammatory responses to myocardial ischemia/reperfusion injury.(29) MI is associated with an accumulation of lymphocytes such as CD4^{+}T and CD8^{+}T cells in damaged myocardium,(29) and inhibition of T cells by cyclosporine A and tacrolimus has been demonstrated to protect the heart against ischemia/reperfusion injury.(30,31) ASCs are known for immunomodulating effects,(9) and it is interesting to note that the transplantation of ASCs in this study prevented sequestration of circulating CD8^{+}T cells 7 days after MI, thereby preventing the post-MI increase in CD4/CD8 ratio in both the single bolus and the divided dose groups (Fig. 4, Supplemental Fig. 4E,F). This alteration in the balance of the T cell ratio may have contributed to the limitation of myocardial injury by ASC.

There are a few limitations in this study. We injected xenogeneic ASCs to allow specific evaluation of the effect of human ASCs in this large animal model of infarction. While we correctly anticipated that xenogeneic ASC transplant would be tolerable given the immunomodulatory effects of this cell type, we recognize the remaining uncertainty whether allogeneic or autologous ASCs might provide greater functional rescue than xenogeneic

Author Manuscript Author Manuscript Author Manuscript Author Manuscript

ASCs. We used 15×10^7 hASCs based on pilot dose escalation studies involving direct coronary artery infusion, and it is unknown whether systemic injection of higher number of ASCs could provide superior improvement in damaged myocardium. Moreover, the follow-up duration was 28 days in this study, and a long-term follow-up could be conducted to confirm a sustained benefit from ASC therapy. We could not use fresh, uncultured cells in this study because not enough hASC could be obtained for intravenous injections in swine myocardial infarction model, and proliferative and differentiation abilities of stem cells gradually decrease at their later passages.

CONCLUSIONS

Data from Phase I clinical trials such as the APOLLO(32) and the PRECISE trials(33) have been presented recently. The APOLLO trial in 14 patients with ST-elevation MI showed a reduction in infarct size after intracoronary injection of autologous ASCs.(32) The PRECISE trial in 27 patients with non-revascularizable ischemic myocardium showed a reduction in infarct size after direct injection of autologous ASCs.(33) These 2 clinical trials used invasive intracoronary and intramyocardial delivery methods. Our preclinical study suggests that noninvasive intravenous delivery of ASCs may also prove effective and feasible in ameliorating ischemia/reperfusion induced myocardial damage, and represents an attractive noninvasive approach that will expand the potential clinical application of ASC therapy for myocardial tissue rescue in patients with acute MI.

Supplementary Material

Refer to Web version on PubMed Central for supplementary material.

Acknowledgments

We thank Michele Schlegelmilch for editorial assistance.

FUNDING SOURCES

This work was supported by National Institutes of Health grants R01 HL077688 (KLM), VA Merit Review Award (KLM), the Cryptic Masons' Medical Research Foundation, and the IUPUI Signature Center for Vascular and Cardiac Adult Stem Cell Therapy.

References

1. Rosamond W, Flegal K, Furie K, Go A, Greenlund K, Haase N, Hailpern SM, Ho M, Howard V, Kissela B, et al. Heart disease and stroke statistics--2008 update: a report from the American Heart Association Statistics Committee and Stroke Statistics Subcommittee. Circulation. 2008; 117:e25–146. [PubMed: 18086926]
2. Menasche P, Hagege AA, Vilquin JT, Desnos M, Abergel E, Pouzet B, Bel A, Sarateanu S, Scorsin M, Schwartz K, et al. Autologous skeletal myoblast transplantation for severe postinfarction left ventricular dysfunction. J Am Coll Cardiol. 2003; 41:1078–83. [PubMed: 12679204]
3. Pagani FD, DerSimonian H, Zawadzka A, Wetzel K, Edge AS, Jacoby DB, Dinsmore JH, Wright S, Aretz TH, Eisen HJ, et al. Autologous skeletal myoblasts transplanted to ischemia-damaged myocardium in humans. Histological analysis of cell survival and differentiation. J Am Coll Cardiol. 2003; 41:879–88. [PubMed: 12628737]
4. Assmus B, Schachinger V, Teupe C, Britten M, Lehmann R, Dobert N, Grunwald F, Aicher A, Urbich C, Martin H, et al. Transplantation of Progenitor Cells and Regeneration Enhancement in

Author Manuscript Author Manuscript Author Manuscript Author Manuscript

Acute Myocardial Infarction (TOPCARE-AMI). Circulation. 2002; 106:3009–17. [PubMed: 12473544]

5. Perin EC, Dohmann HF, Borojevic R, Silva SA, Sousa AL, Mesquita CT, Rossi MI, Carvalho AC, Dutra HS, Dohmann HJ, et al. Transendocardial, autologous bone marrow cell transplantation for severe, chronic ischemic heart failure. Circulation. 2003; 107:2294–302. [PubMed: 12707230]
6. Wollert KC, Meyer GP, Lotz J, Ringes-Lichtenberg S, Lippolt P, Breidenbach C, Fichtner S, Korte T, Hornig B, Messinger D, et al. Intracoronary autologous bone-marrow cell transfer after myocardial infarction: the BOOST randomised controlled clinical trial. Lancet. 2004; 364:141–8. [PubMed: 15246726]
7. Kang HJ, Lee HY, Na SH, Chang SA, Park KW, Kim HK, Kim SY, Chang HJ, Lee W, Kang WJ, et al. Differential effect of intracoronary infusion of mobilized peripheral blood stem cells by granulocyte colony-stimulating factor on left ventricular function and remodeling in patients with acute myocardial infarction versus old myocardial infarction: the MAGIC Cell-3-DES randomized, controlled trial. Circulation. 2006; 114:I145–51. [PubMed: 16820564]
8. Kim YS, Ahn Y. A long road for stem cells to cure sick hearts: update on recent clinical trials. Korean Circ J. 2012; 42:71–9. [PubMed: 22396692]
9. Hong SJ, Traktuev DO, March KL. Therapeutic potential of adipose-derived stem cells in vascular growth and tissue repair. Curr Opin Organ Transplant. 2010; 15:86–91. [PubMed: 19949335]
10. Hong SJ, Kihlken J, Choi SC, March KL, Lim DS. Intramyocardial transplantation of human adipose-derived stromal cell and endothelial progenitor cell mixture was not superior to individual cell type transplantation in improving left ventricular function in rats with myocardial infarction. Int J Cardiol. 2013; 164:205–11. [PubMed: 21794931]
11. Hong SJ, Hou D, Brinton TJ, Johnstone B, Feng D, Rogers P, Fearon WF, Yock P, March KL. Intracoronary and retrograde coronary venous myocardial delivery of adipose-derived stem cells in swine infarction lead to transient myocardial trapping with predominant pulmonary redistribution. Catheter Cardiovasc Interv. 2014; 83:E17–25. [PubMed: 22972685]
12. Schweitzer KS, Johnstone BH, Garrison J, Rush NI, Cooper S, Traktuev DO, Feng D, Adamowicz JJ, Van Demark M, Fisher AJ, et al. Adipose stem cell treatment in mice attenuates lung and systemic injury induced by cigarette smoking. Am J Respir Crit Care Med. 2011; 183:215–25. [PubMed: 20709815]
13. Hou D, Youssef EA, Brinton TJ, Zhang P, Rogers P, Price ET, Yeung AC, Johnstone BH, Yock PG, March KL. Radiolabeled cell distribution after intramyocardial, intracoronary, and interstitial retrograde coronary venous delivery: implications for current clinical trials. Circulation. 2005; 112:I150–6. [PubMed: 16159808]
14. Hong SJ, Choi SC, Kim JS, Shim WJ, Park SM, Ahn CM, Park JH, Kim YH, Lim DS. Low-dose versus moderate-dose atorvastatin after acute myocardial infarction: 8-month effects on coronary flow reserve and angiogenic cell mobilisation. Heart. 2010; 96:756–64. [PubMed: 20448126]
15. Ahn CM, Hong SJ, Choi SC, Park JH, Kim JS, Lim DS. Red ginseng extract improves coronary flow reserve and increases absolute numbers of various circulating angiogenic cells in patients with first ST-segment elevation acute myocardial infarction. Phytother Res. 2011; 25:239–249. [PubMed: 20641058]
16. Traktuev DO, Prater DN, Merfeld-Clauss S, Sanjeevaiah AR, Saadatzadeh MR, Murphy M, Johnstone BH, Ingram DA, March KL. Robust functional vascular network formation in vivo by cooperation of adipose progenitor and endothelial cells. Circ Res. 2009; 104:1410–20. [PubMed: 19443841]
17. Kaufmann BA, Carr CL, Belcik T, Xie A, Kron B, Yue Q, Lindner JR. Effect of acoustic power on in vivo molecular imaging with targeted microbubbles: implications for low-mechanical index real-time imaging. J Am Soc Echocardiogr. 2010; 23:79–85. [PubMed: 19910159]
18. Ince H, Petzsch M, Kleine HD, Schmidt H, Rehders T, Korber T, Schumichen C, Freund M, Nienaber CA. Preservation from left ventricular remodeling by front-integrated revascularization and stem cell liberation in evolving acute myocardial infarction by use of granulocyte-colony-stimulating factor (FIRSTLINE-AMI). Circulation. 2005; 112:3097–106. [PubMed: 16275869]
19. Schiller NB, Shah PM, Crawford M, DeMaria A, Devereux R, Feigenbaum H, Gutgesell H, Reichek N, Sahn D, Schnittger I, et al. Recommendations for quantitation of the left ventricle by two-dimensional echocardiography. American Society of Echocardiography Committee on

Author Manuscript Author Manuscript Author Manuscript Author Manuscript

Standards, Subcommittee on Quantitation of Two-Dimensional Echocardiograms. J Am Soc Echocardiogr. 1989; 2:358–67. [PubMed: 2698218]

20. Lee RH, Pulin AA, Seo MJ, Kota DJ, Ylostalo J, Larson BL, Semprun-Prieto L, Delafontaine P, Prockop DJ. Intravenous hMSCs improve myocardial infarction in mice because cells embolized in lung are activated to secrete the anti-inflammatory protein TSG-6. Cell Stem Cell. 2009; 5:54–63. [PubMed: 19570514]
21. Cai L, Johnstone BH, Cook TG, Tan J, Fishbein MC, Chen PS, March KL. IFATS collection: Human adipose tissue-derived stem cells induce angiogenesis and nerve sprouting following myocardial infarction, in conjunction with potent preservation of cardiac function. Stem Cells. 2009; 27:230–7. [PubMed: 18772313]
22. Sharif F, Bartunek J, Vanderheyden M. Adult stem cells in the treatment of acute myocardial infarction. Catheter Cardiovasc Interv. 2011; 77:72–83. [PubMed: 20506335]
23. Kang HJ, Kim HS, Zhang SY, Park KW, Cho HJ, Koo BK, Kim YJ, Soo Lee D, Sohn DW, Han KS, et al. Effects of intracoronary infusion of peripheral blood stem-cells mobilised with granulocyte-colony stimulating factor on left ventricular systolic function and restenosis after coronary stenting in myocardial infarction: the MAGIC cell randomised clinical trial. Lancet. 2004; 363:751–6. [PubMed: 15016484]
24. Danchuk S, Ylostalo JH, Hossain F, Sorge R, Ramsey A, Bonvillain RW, Lasky JA, Bunnell BA, Welsh DA, Prockop DJ, et al. Human multipotent stromal cells attenuate lipopolysaccharide-induced acute lung injury in mice via secretion of tumor necrosis factor-alpha-induced protein 6. Stem Cell Res Ther. 2011; 2:27. [PubMed: 21569482]
25. Agarwal U, Ghalayini W, Dong F, Weber K, Zou YR, Rabbany SY, Rafii S, Penn MS. Role of cardiac myocyte CXCR4 expression in development and left ventricular remodeling after acute myocardial infarction. Circ Res. 2010; 107:667–76. [PubMed: 20634485]
26. Mannaerts HF, van der Heide JA, Kamp O, Stoel MG, Twisk J, Visser CA. Early identification of left ventricular remodelling after myocardial infarction, assessed by transthoracic 3D echocardiography. Eur Heart J. 2004; 25:680–7. [PubMed: 15084373]
27. Dong F, Khalil M, Kiedrowski M, O'Connor C, Petrovic E, Zhou X, Penn MS. Critical role for leukocyte hypoxia inducible factor-1alpha expression in post-myocardial infarction left ventricular remodeling. Circ Res. 2010; 106:601–10. [PubMed: 20035082]
28. Sim DS, Jeong MH, Cho KH, Ahn Y, Kim YJ, Chae SC, Hong TJ, Seong IW, Chae JK, Kim CJ, et al. Effect of early statin treatment in patients with cardiogenic shock complicating acute myocardial infarction. Korean Circ J. 2013; 43:100–9. [PubMed: 23508129]
29. Murray DR, Polizzi SM, Harris TJ, Maisel AS. Myocardial ischemia alters immunoregulatory cell traffic and function in the rat independent of exogenous catecholamine administration. J Neuroimmunol. 1996; 71:107–13. [PubMed: 8982109]
30. Squadrito F, Altavilla D, Squadrito G, Saitta A, Campo GM, Arlotta M, Quartarone C, Ferlito M, Caputi AP. Cyclosporin-A reduces leukocyte accumulation and protects against myocardial ischaemia reperfusion injury in rats. Eur J Pharmacol. 1999; 364:159–68. [PubMed: 9932719]
31. Squadrito F, Altavilla D, Squadrito G, Saitta A, Deodato B, Arlotta M, Minutoli L, Quartarone C, Ferlito M, Caputi AP. Tacrolimus limits polymorphonuclear leucocyte accumulation and protects against myocardial ischaemia- reperfusion injury. J Mol Cell Cardiol. 2000; 32:429–40. [PubMed: 10731442]
32. Houtgraaf JH, den Dekker WK, van Dalen BM, Springeling T, de Jong R, van Geuns RJ, Geleijnse ML, Fernandez-Aviles F, Zijlsta F, Serruys PW, et al. First experience in humans using adipose tissue-derived regenerative cells in the treatment of patients with ST-segment elevation myocardial infarction. J Am Coll Cardiol. 2012; 59:539–40. [PubMed: 22281257]
33. Perin EC, Sanchez PL, Ruiz RS, Perez-Cano R, Lasso J, Alonso-Farto JC, Fernandez-Pina L, Serruys PW, Duckers HJ, Kastrup J, et al. Abstract 17966: First In Man Transendocardial Injection of Autologous AdiPose-deRived StEm Cells in Patients with Non RevaScularizable IschEmic Myocardium (PRECISE). Circulation. 2010; 122:A17966.

Author Manuscript Author Manuscript Author Manuscript Author Manuscript

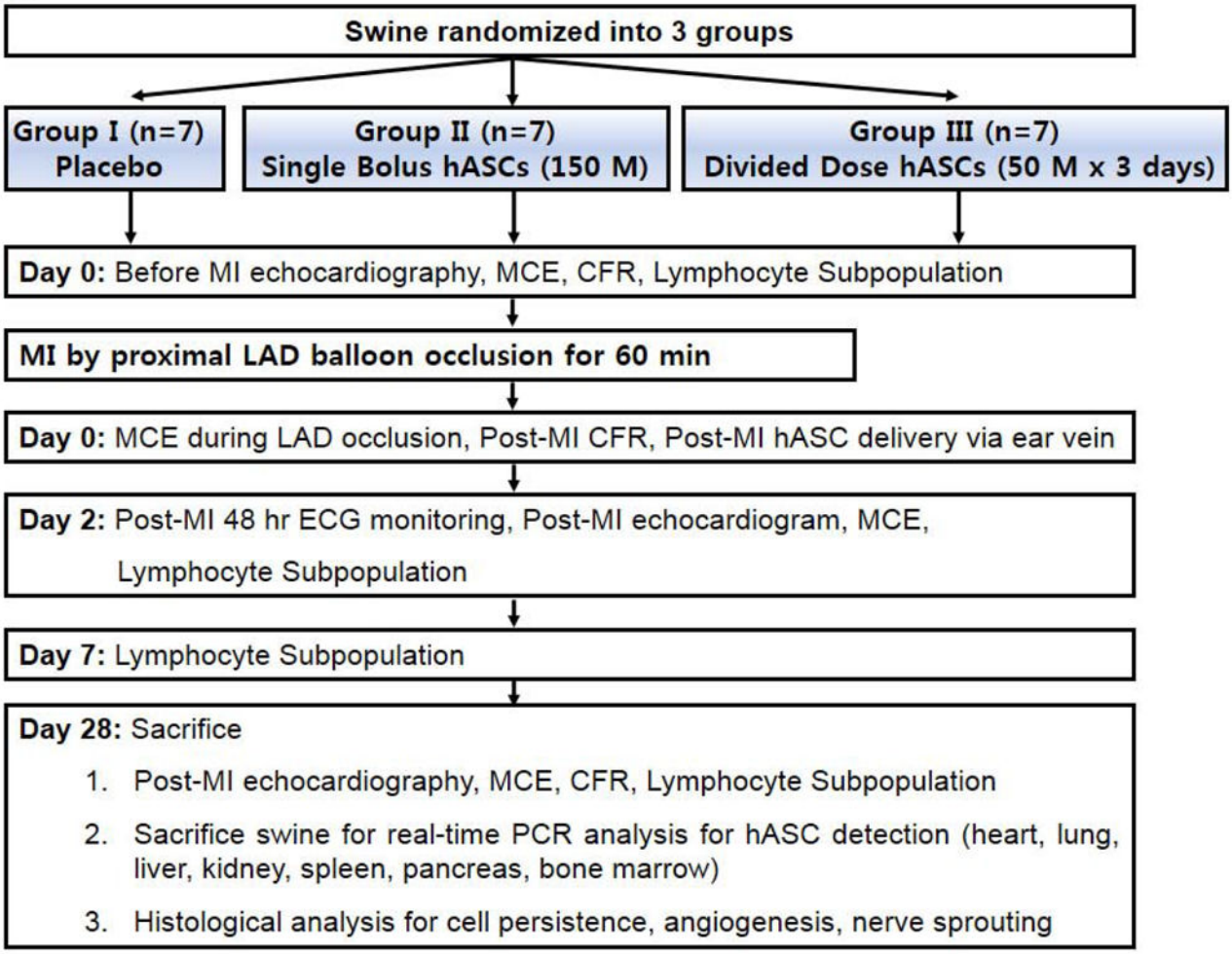

Fig. 1.

Study protocol. Swine were randomized into 3 groups (placebo, single bolus, and divided dose). Echocardiography, MCE, CFR, lymphocyte subpopulation analysis were done before MI and 2 and 28 days after MI. CFR was measured before MI, 2 hrs and 28 days after MI.

Author Manuscript Author Manuscript Author Manuscript Author Manuscript

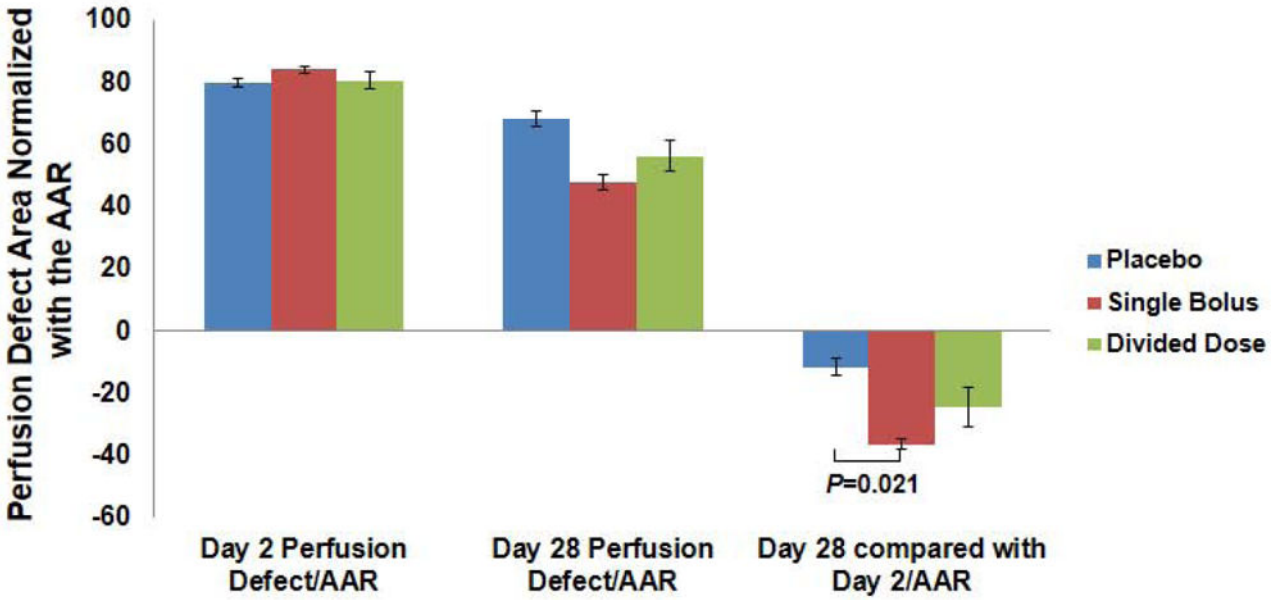

Fig. 2.

The perfusion defect area was normalized with the baseline AAR, and the decrease in the perfusion defect area from day 2 to day 28 was significantly greater in the single bolus group compared to the placebo group.

Author Manuscript Author Manuscript Author Manuscript Author Manuscript

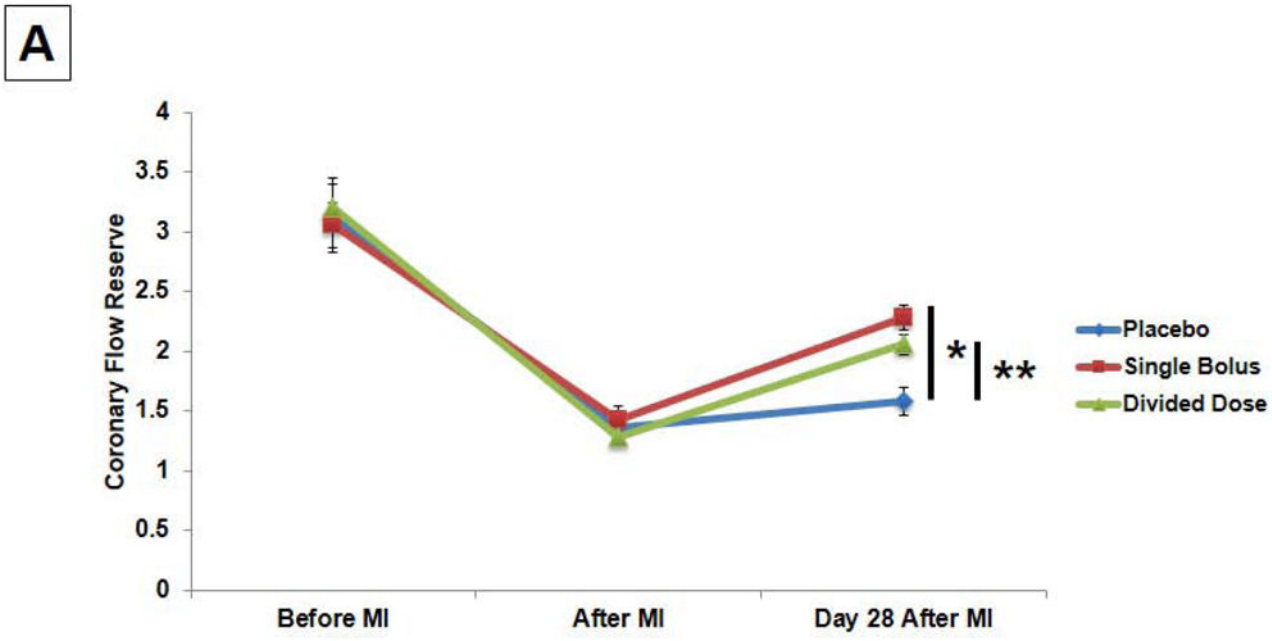

Author Manuscript Author Manuscript Author Manuscript Author Manuscript

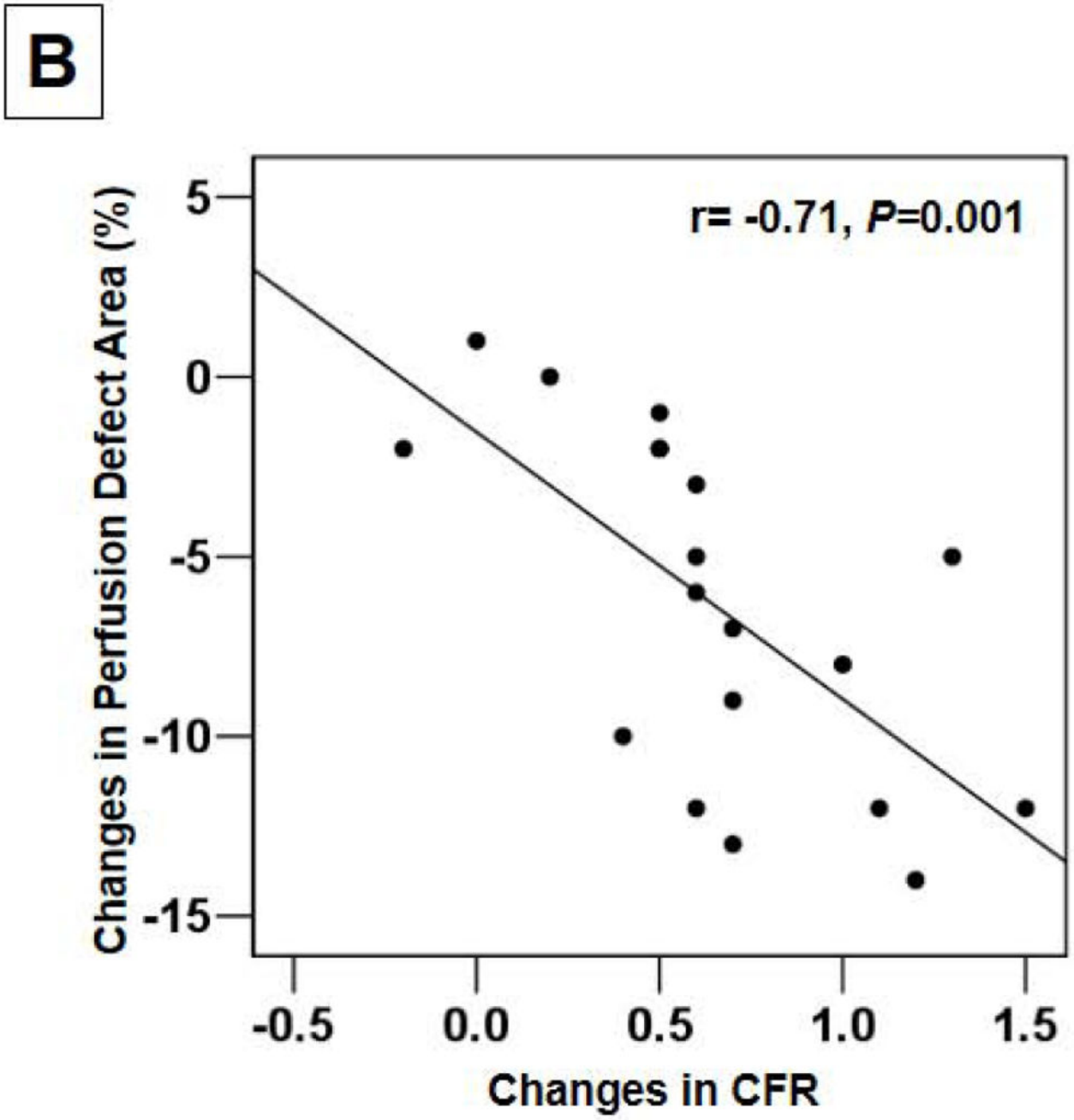

Fig. 3.

(A) CFR revealed significant increases in the single bolus and the divided dose groups than the placebo group (**P*<0.01 and ***P*<0.05). (B) The decreases in the perfusion defect area (%) during the follow-up correlated with the increases in CFR.

Author Manuscript Author Manuscript Author Manuscript Author Manuscript

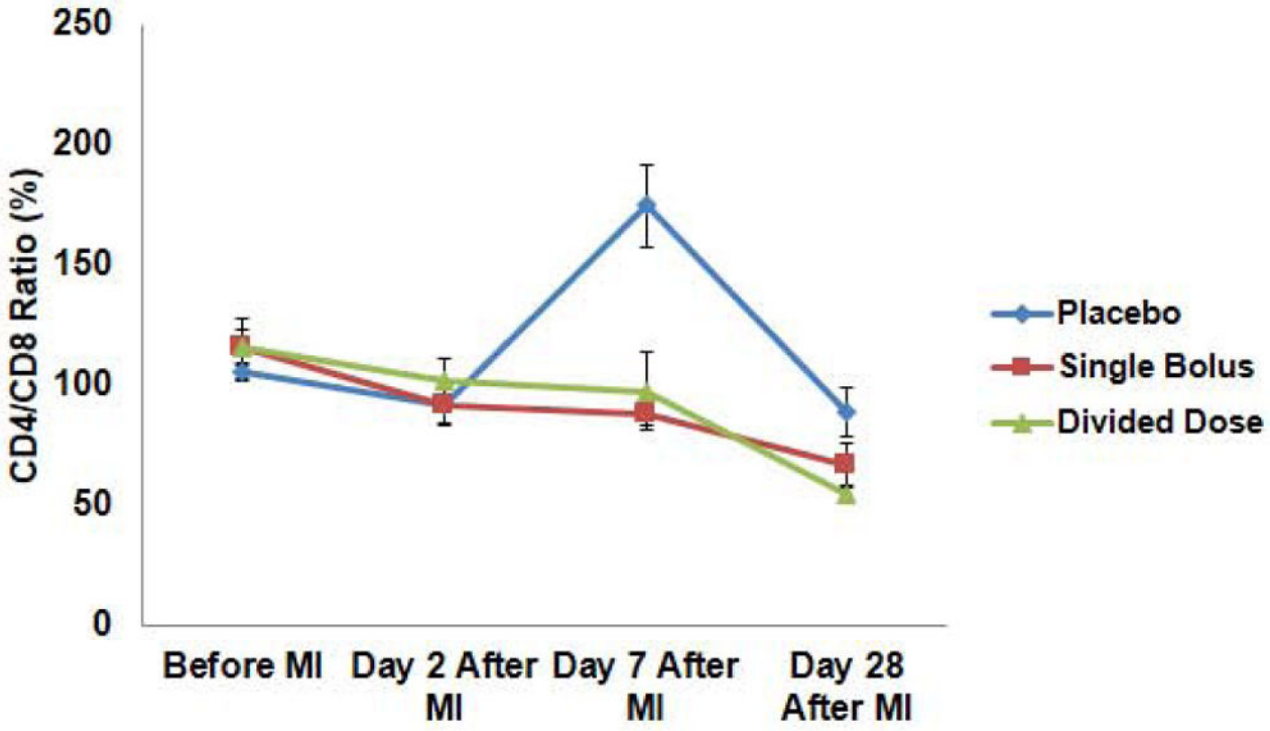

Fig. 4.

Serial changes in CD4/CD8 ratio in the placebo group showed significant increases when compared to the single bolus and the divided dose groups (P=0.016).

Author Manuscript Author Manuscript Author Manuscript Author Manuscript

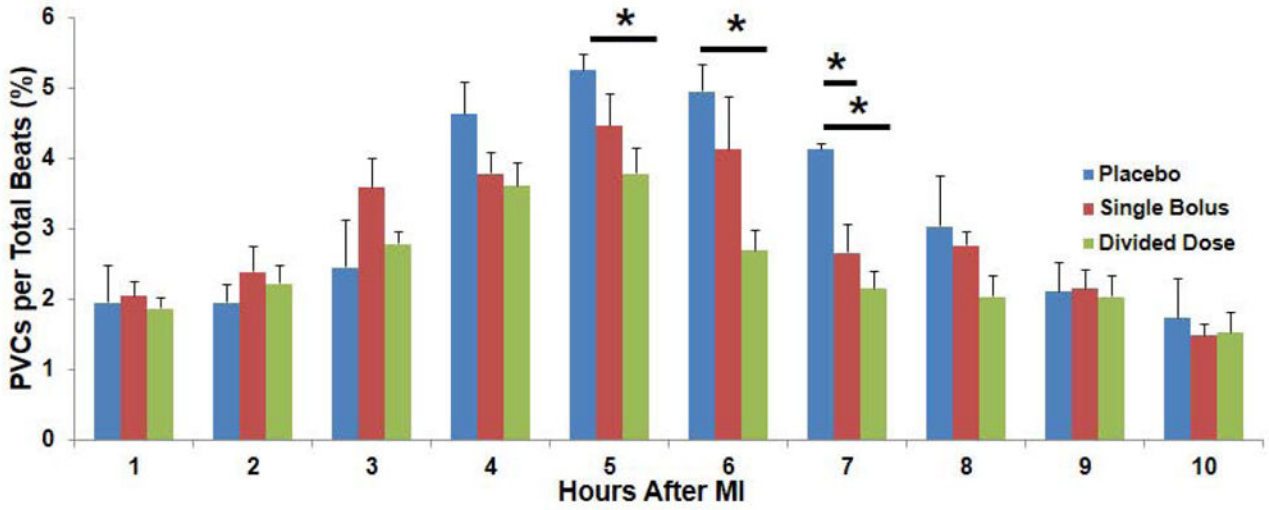

Fig. 5.

PVCs(%) in each hour after MI. Most of PVCs occurred within 10 hours after MI, and the serial changes in PVCs(%) in the single bolus and divided dose groups showed significant decreases when compared to the placebo group especially at 5, 6, and 7 hours after MI (*P<0.05).

Author Manuscript
Author Manuscript
Author Manuscript
Author Manuscript

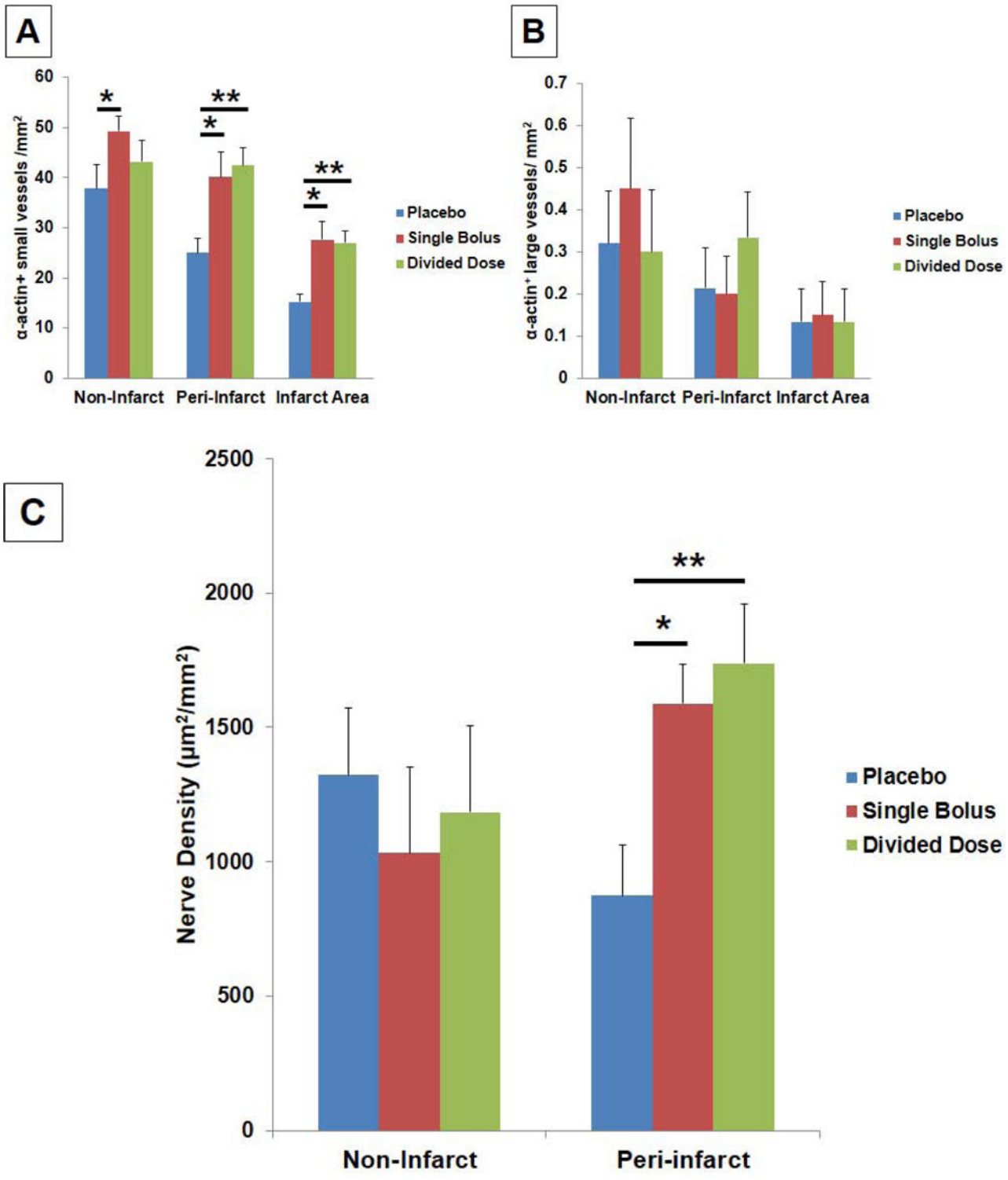

Fig. 6.

(A) Significant increases in the number of ±-actin+ small and collapsed vessels were found in the single bolus group in the non-infarct (*P<0.05), peri-infarct (*P<0.05), and infarct areas (*P<0.05). Significant increases in the number of ±-actin+ small and collapsed vessels

Author Manuscript Author Manuscript Author Manuscript Author Manuscript

were also found in the divided dose group in the peri-infarct (**P<0.01) and infarct areas (**P<0.01). (B) No significant differences in the number of ±-actin+ large vessels were found among 3 groups. (C) Significant increases in the GAP43+ nerve density were found in the single bolus (*P<0.05) and the divided dose group (**P=0.005) when compared to the placebo group in the peri-infarct areas.

Author Manuscript Author Manuscript Author Manuscript Author Manuscript

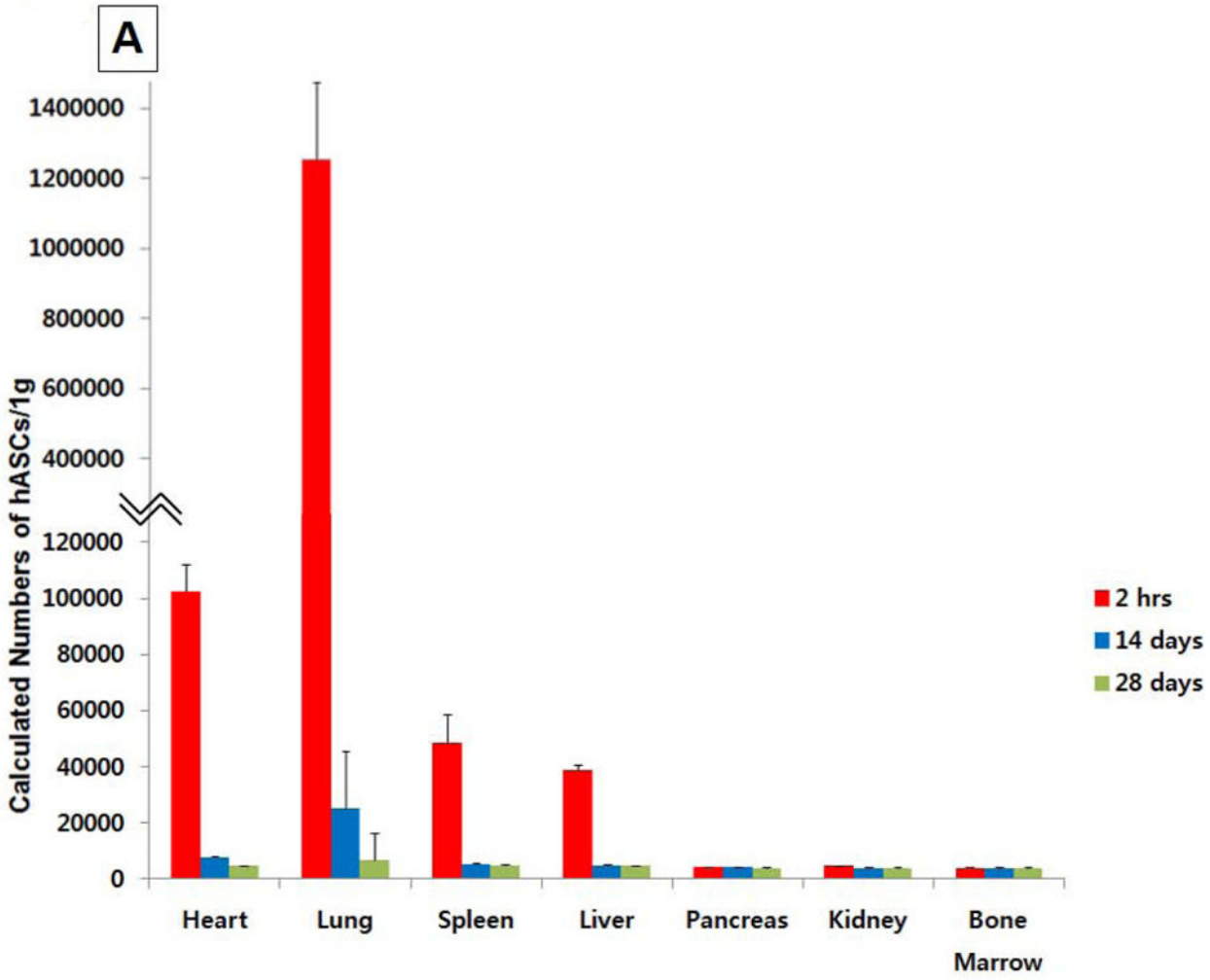

Author Manuscript Author Manuscript Author Manuscript Author Manuscript

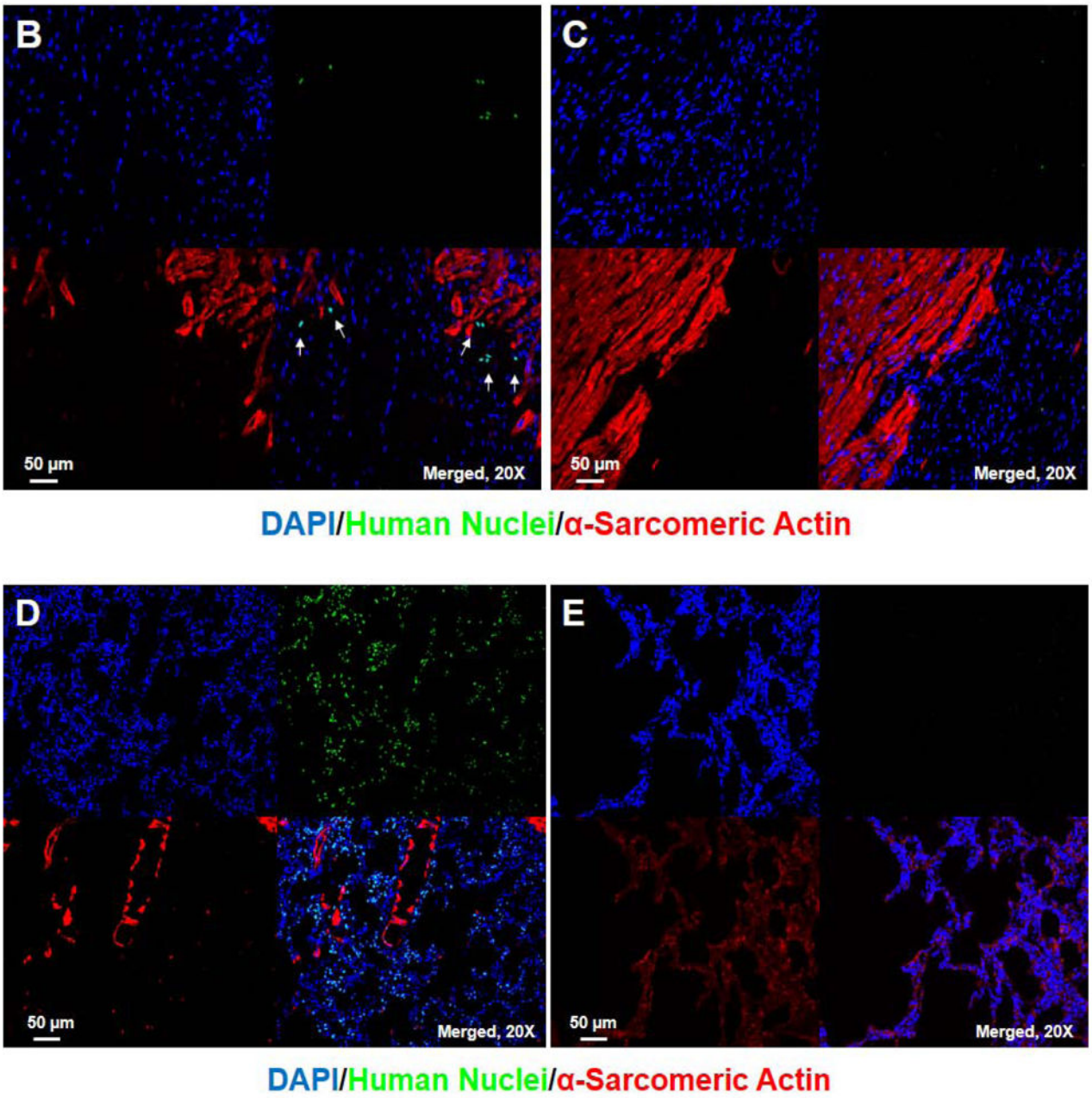

Fig. 7.

Tissue distribution after systemic injection of 15×10^7 hASCs. (A) More than 85% of hASCs were found in the lung 2 hour after intravenous injection, and no large number of hASCs was detected 14 days after intravenous injections. (B) Identification of hASC presence by immunostaining (20x) in the periinfarct area 2 hours after intravenous injection of 15×10^7 cells. Bars=50μm. (C) No hASCs were found in the heart 28 days after intravenous injection. (D) hASCs were present in the interstitial space in the lung 2 hours after intravenous injection of 15×10^7 cells. (E) No human ASCs were found in the lung 28 days after intravenous injection.

Author Manuscript

Author Manuscript

Author Manuscript

Author Manuscript

Table 1

Comparison of the Body Weight, Troponin-I, and Echocardiographic Parameters

	Placebo	Single Bolus	Divided Dose	*P* value
Weight, kg	31.2±1.0	34.9±1.7	32.6±1.3	0.193
Troponin-I at Day 2, ng/mL	96.4±25.5	90.0±18.7	108.6±5.1	0.695
LVEF before MI, %	64.0±1.0	65.7±1.1	64.6±1.3	0.561
LVEF at Day 2, %	41.0±1.1	41.7±0.7	39.6±0.8	0.162
LVEF at Day 28, %	40.6±1.3	47.1±1.1	43.3±1.0	0.010
Change in LVEF from Day 0 to 2, %	-23.0±1.5	-24.0±1.3	-25.0±1.9	0.594
Change in LVEF from Day 2 to 28, %	-0.4±0.6	5.4±0.9	3.7±0.7	0.003
Anterior Wall Thickening at Day 28, %	21.6±7.5	44.1±3.2	30.1±2.4	0.019
Inferior Wall Thickening at Day 28, %	66.2±4.1	70.0±3.7	62.7±1.8	0.386
Anterior/Inferior Thickening Ratio at Day 28	31.5±10.2	63.2±4.0	47.8±3.3	0.012
Wall Motion Score Index (WMSI) at Day 2	1.71±0.21	1.70±0.18	1.74±0.25	0.949
Wall Motion Score Index (WMSI) at Day 28	1.70±0.17	1.38±0.11	1.35±0.12	0.001